

## High energy $\gamma$ rays from $^{252}\text{Cf}$ spontaneous fission

D. J. Hofman, B. B. Back,\* C. P. Montoya, S. Schadmand, R. Varma,  
and P. Paul

*Department of Physics, State University of New York at Stony Brook, Stony Brook, New York 11794*

(Received 12 November 1992)

The spontaneous fission decay of  $^{252}\text{Cf}$  has been analyzed in a statistical model with emphasis on describing recently reported high energy  $\gamma$ -ray spectra. An enhanced  $\gamma$  emission in the range from 3 to 10 MeV which is observed for nearly symmetric mass splits is readily understood as a result of the different fragment excitation energies. The model includes a viscous motion to the scission point with the possibility of pre-scission  $\gamma$  emission. It was found that even with saddle-to-scission times of  $\tau_{sc} < 66 \times 10^{-19}$  s, the maximum consistent with pre-scission neutron multiplicities, pre-scission  $\gamma$  rays are overwhelmed by fragment  $\gamma$  rays. Thus, the recently reported strong angular anisotropy of  $\gamma$  rays in the range  $E_\gamma = 8\text{--}12$  MeV is unexplained within the present understanding of the fission process.

PACS number(s): 25.85.Ca, 27.90.+b

### I. INTRODUCTION

Recent measurements have reported high energy  $\gamma$ -ray spectra emitted in the spontaneous fission of  $^{252}\text{Cf}$  which show several surprising features. Van der Ploeg *et al.* [1] observe  $\gamma$  rays up to about 15 MeV and an enhanced emission of  $\gamma$  rays with energies around 10 MeV in the direction of the fission axis. Glässel *et al.* [2] and then Wiswesser *et al.* [3] report the  $^{252}\text{Cf}$   $\gamma$  spectrum up to about 10 MeV as a function of fission mass asymmetry, showing a significant enhancement in the region from 3 to 8 MeV for symmetric fission events.

In spontaneous fission, high energy  $\gamma$  rays are emitted by the excited fission fragments, but possibly also by the fissioning nucleus on its path from the saddle to the scission point. Recent measurements of high-energy  $\gamma$  rays from the decay of hot ( $T \sim 2.0$  MeV) thorium nuclei [4, 5] have found that high-energy  $\gamma$  rays are indeed emitted both before and after traversing the saddle point, and that these provide information about the dynamics of the fission process. Specifically, it was concluded from the strong presence of pre-scission  $\gamma$  rays that the fission mass motion was strongly overdamped, with a normalized nuclear friction coefficient of  $\gamma=10$ , corresponding to a fission time scale  $\sim 10^{-19}$  s. Here,  $\gamma = \beta/2\omega_0$ , where  $\beta$  is the reduced friction coefficient and  $\omega_0$  is a characteristic potential or barrier curvature.

In this paper we analyze the spontaneous fission- $\gamma$  data of Refs. [1, 3] using the same formalism as in the analysis of the hot Th fission, with the aim to see if any of the interesting results cited above may be related to  $\gamma$  rays emitted from the fissioning system on its way from the saddle to the scission point. Calculations by Nix and

Sierk [6] of the kinetic energy of fission fragments resulting from  $^{252}\text{Cf}$  at a temperature  $T = 2.0$  MeV have shown that the amount of damping in the saddle-to-scission mass motion results in scission time scales which vary from  $2 \times 10^{-21}$  s for no dissipation to  $30 \times 10^{-21}$  s for full one-body dissipation (corresponding to the wall-window formula). This time is long enough to allow the emission of giant dipole resonance (GDR)  $\gamma$  rays.

### II. ANALYSIS OF FRAGMENT DECAY

To calculate the  $\gamma$  spectrum and the  $\gamma$  yield per fission event, as well as the  $\gamma$ -fission angular correlation we use a modified version of the statistical code CASCADE [7] which includes the fission process with friction and GDR  $\gamma$  emission on the path from saddle to scission [4], as well as from the fission fragments [8]. In order to constrain the parameters of the model as much as possible we require that the calculations reproduce the wealth of data that are available on  $^{252}\text{Cf}$ . The most prominent feature of spontaneous fission of  $^{252}\text{Cf}$  is the strongly asymmetric mass distribution caused by the shell structure of the nascent fragments near the scission point [9]. The present calculations use the experimental data for the mass distribution, as well as the mean and variance of the kinetic energy distribution measured as a function of fragment mass [10, 11]. The total excitation energy available for statistical decay of the fragments is given by the energy balance

$$E^*(A_{\text{frag}}) = Q(A_{\text{frag}}) - E_K(A_{\text{frag}})$$

where the *total* excitation energy  $E^*$ , the fission  $Q$  value  $Q$ , and the total kinetic energy  $E_K$  depend on the mass  $A_{\text{frag}}$  of one of the fragments.

For each fragment mass  $A_{\text{frag}}$  a charge number is needed to look up the experimental fission  $Q$  value  $Q(A_{\text{frag}})$ . These were assumed to follow the uniform charge distribution [14, 15], i.e.,  $Z_{\text{frag}} = A_{\text{frag}}98/252$ .

\*On leave from Argonne National Laboratory, Argonne, IL 60439.

This is identical, within one-half charge unit, to the charge division expected from the liquid drop model for a fixed mass division between two touching fragments.

The excitation energy in the fragments after scission originates from two sources: (1) the excitation energy of the system at scission and (2) the deformation energy of each fragment at or near the scission point which is converted to excitation energy shortly after separation. Assuming a uniform temperature at scission, the excitation energy at that point is divided according to the fragment mass. Thus, the (average) excitation energy of a fragment is given by

$$E_1^* = E_1^{\text{def}} + \frac{A_1}{A_1 + A_2}(Q - E_K - E_1^{\text{def}} - E_2^{\text{def}}) - E_1^{\text{rot}},$$

where  $E_1^{\text{def}}$  and  $E_2^{\text{def}}$  are the fragment deformation energies at the scission point, and the rotational energy,  $E_1^{\text{rot}}$ , is calculated for an average fragment angular momentum  $J = 6\hbar$  [16]. The fragment scission point deformations,  $\beta(A_{\text{frag}})$ , were taken from Ref. [9], and the corresponding deformation potentials were calculated from the liquid-drop model by including the Coulomb and surface energy terms [17]. The excitation energy of the complementary fragment with mass  $A_2$  is obtained analogously. The measured total kinetic energy shows an experimental variance which translates directly into a variance of the total excitation energy  $E^*$ , i.e.,  $\sigma_{E^*}^2(A_{\text{frag}}) = \sigma_{E_K}^2(A_{\text{frag}})$ , since the fission  $Q$  value has a negligible variance or experimental uncertainty. There is very little experimental evidence on how  $\sigma_{E^*}^2$  is split between the two fragments, but it can be argued that the covariance of the two energy distributions is negligible [18], as we will assume here. Even with this constraint it is necessary to make an assumption about the distribution of the excitation energy variance, and we assume that the variance in each fragment scales directly with its excitation energy, i.e.,

$$\sigma_{E_1^*}^2 = \frac{E_1^*}{E_1^* + E_2^*} \sigma_{E^*}^2.$$

Because of the zero covariance we can perform independent calculations for each fragment and then add the contributions.

The level density parameter as a function of fragment mass,  $a(A_{\text{frag}})$ , was taken from the measurements of Ref. [11], where  $a$  was extracted directly from the slope of the mass-gated neutron energy spectra. The energy offset  $\Delta$  in the level density was set equal to zero since  $a$  was measured independently of the fragment charges, thus including and averaging over the pairing energy effects.

The CASCADE results for neutrons emitted by the fission fragments which were obtained with this input are compared to the corresponding measured quantities in Fig. 1. The striking mass dependence of the average neutron multiplicity (top panel) is well reproduced by the calculation. The observed sawtooth behavior is related to the shell structure of the nascent fragments at the scission point. The average neutron energy (center panel) is also well described. Finally, the neutron temperatures are compared with the data in the bottom panel. The fit

is very good for light and symmetric masses, but poorer for heavy masses. This could not be improved within our model, without destroying the quality of the fits in panels (a) and (b). The poor fit may result from the fact that the calculated neutron spectra are not strictly exponentials. However, on the whole, these fits give confidence that the present prescription for the excitation energy of the fission fragments provides a realistic basis for calculating the emission probability of high energy  $\gamma$  rays.

The calculation of the high energy  $\gamma$ -ray spectrum assumes the usual GDR dominance with a strength function

$$F(E_\gamma) = S \frac{\Gamma_{\text{GDR}} E_\gamma^4}{(E_\gamma^2 - E_{\text{GDR}}^2)^2 + (\Gamma_{\text{GDR}} E_\gamma)^2}.$$

Here  $S$  is the overall strength in units of the classical sum rule,  $E_{\text{GDR}}$  is the energy, and  $\Gamma_{\text{GDR}}$  the width of the giant dipole resonance. For the fragments, we take from

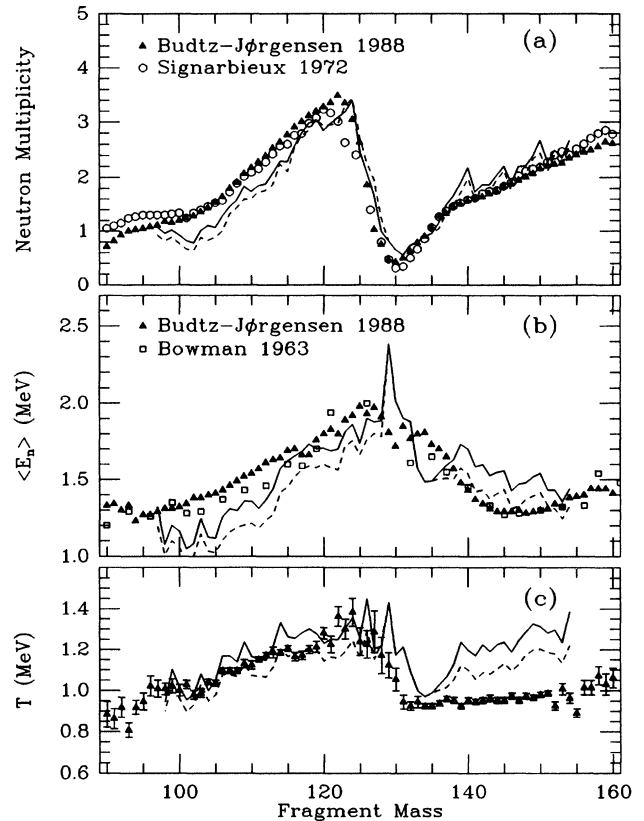


FIG. 1. Comparisons of CASCADE calculations (solid curves) to experimental data (solid triangles [11], open circles [12], open squares [13]) for neutron emission in  $^{252}\text{Cf}$  spontaneous fission. (a) The neutron multiplicity, (b) average neutron energy,  $\langle E_n \rangle$ , and (c) the nuclear temperature extracted from both the calculated and measured neutron spectra are shown. The overprediction of the temperature for heavy fragments [see (c)] is possibly caused by a nonexponential character of the calculated spectra. Note the offset scale in (b) and (c). The dashed curve represents a fit assuming a reduced initial excitation energy (see text).

experiments in the Sn region [19] that  $S = 1$ ,  $E_{\text{GDR}} = 79A^{-1/3}$ , and  $\Gamma_{\text{GDR}} = 4.8 + 0.0026(E_{\text{frag}}^*)^{1.6}$ .

Figure 2 shows the corresponding calculated  $\gamma$  energy spectra emitted by the fragments together with the experimental results of van der Ploeg *et al.* [1] and earlier measurements [20–22]. The overall  $\gamma$  spectrum shape and yield are well reproduced; however, the  $\gamma$  yield above 10 MeV is strongly overpredicted. These  $\gamma$  rays come from the first decay steps of the fragments and the discrepancy could be decreased by lowering the *initial* fragment excitation energy. Within the tight experimental constraints, this might be explained if the relaxation time of the various collective vibrational modes excited during the scission process is of the same order as the emission time of the first neutron (a questionable assumption). We have explored this possibility by (arbitrarily) scaling down the excitation energies by about 40% ( $\lesssim 7$  MeV) of the deformation energy in the first decay step for each fragment. This calculation is represented by the dashed curves in Figs. 1 and 2. We observe that this modification improves the fit in the high energy region of the  $\gamma$  spectrum (see Fig. 2). However, the agreement with the neutron data is generally reduced as seen in Fig. 1.

The lower part of Fig. 2 shows the measured  $\gamma$ -fission anisotropy and a calculation of the anisotropy produced

by the Doppler shift of the fission-fragment  $\gamma$  rays. Here, it is assumed that the fragments are fully accelerated and the  $\gamma$ -ray yield is isotropic in the fragment rest frame. Then the Doppler anisotropy is simply given by

$$\frac{W_f(0^\circ, E_\gamma)}{W_f(90^\circ, E_\gamma)} = \frac{1}{2} \frac{\sigma_f^{\text{Dopp}+}(E_\gamma) + \sigma_f^{\text{Dopp}-}(E_\gamma)}{\sigma_f(E_\gamma)}$$

where  $0^\circ$  points along the fission axis,  $90^\circ$  is perpendicular to this axis, and  $\sigma_f(E_\gamma)$  is the total calculated fission-fragment  $\gamma$  energy spectrum. The fragment velocities as a function of fragment mass,  $v(A_f)$ , were obtained from the measured fission fragment kinetic energies [10].  $\sigma_f^{\text{Dopp}\pm}$  are the summed fragment  $\gamma$  yields from fragments going towards (+) and away (-) from the  $\gamma$ -ray detector. Obviously, the Doppler shift related anisotropy is both too small and centered at too low an energy to explain the measurement.

We now address the observed strong dependence of the fission  $\gamma$ -ray spectrum on the mass of the fragments [2, 3]. The experiments show a pronounced enhancement in the  $\gamma$  energy region from 3 to 10 MeV when mass-symmetric fission fragments are selected. Dietrich and Bondorf [23] have speculated that this enhancement results from large amplitude vibrations excited in the nascent fission fragments during the scission process. However, Fig. 3 shows

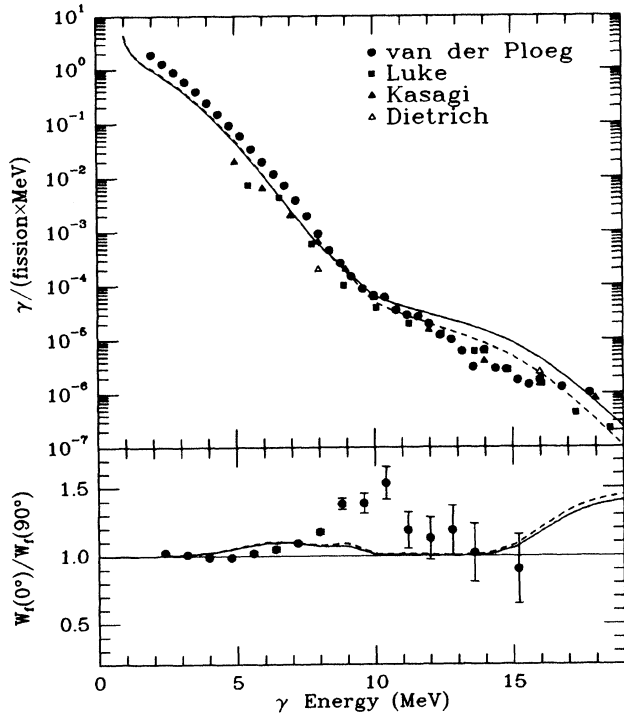


FIG. 2. Top panel: Comparison of the calculated  $\gamma$  spectra (solid curve) to experimental data (filled circles [1], solid squares [20], solid triangles [21], and open triangles [22]). Bottom panel: The calculated anisotropy (solid curve) arising from Doppler shifts is compared to experimental data [1] (filled circles). The dashed curve represents a fit assuming a reduced initial excitation energy (see text).

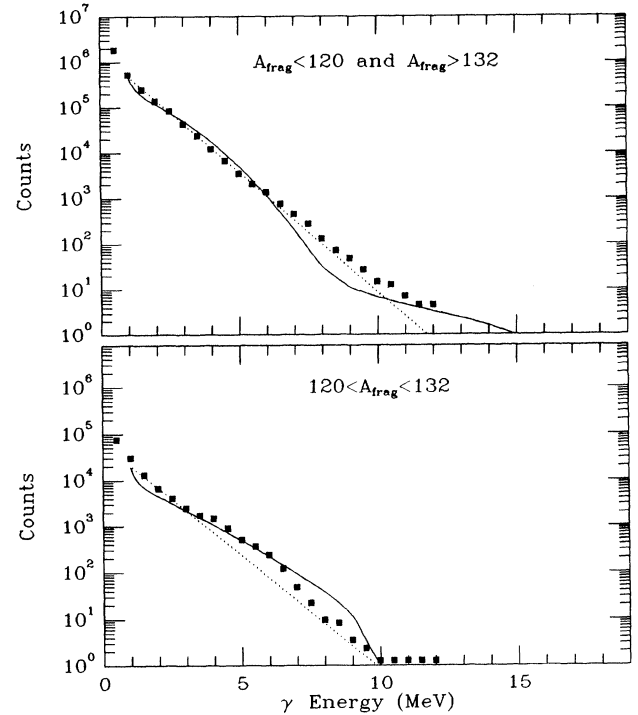


FIG. 3. The calculated (solid curve) gamma-ray spectra for symmetric (bottom panel) and asymmetric (top panel) fission of  $^{252}\text{Cf}$  are compared to experimental data [3] (solid squares). The normalization constant for both calculated spectra was determined from fitting the asymmetric-fission  $\gamma$  spectrum to the  $E_\gamma = 1$  MeV data point. The dotted line represents the exponential background used in Ref. [3].

that our calculation is able to qualitatively reproduce this mass-selective enhancement without introducing any new effect. (A quantitative comparison would require the use of the detector response function of Ref. [3].) The effect arises from the strong mass dependence of the fragment excitation energies and level densities. The average total excitation energy of nearly symmetric fragments ( $120 \leq A_{\text{frag}} \leq 132$ ) is 39.4 MeV with the heavier fragments receiving  $\leq 25\%$  of this energy, whereas the more asymmetric fragments have total average excitation energies of 31.2 MeV divided about evenly between both fragment pairs. Therefore the shoulder at  $E_\gamma \approx 9\text{--}10$  MeV and corresponding enhanced  $\gamma$ -ray yield for  $E_\gamma \approx 3\text{--}10$  MeV is obtained straightforwardly: It is associated with the threshold for second-chance  $\gamma$  emission following initial emission of a neutron for the heavier mass fragments ( $127 \leq A_{\text{frag}} \leq 132$ ) which have reduced excitation energies and lower level densities. Thus it appears that the fragment excitation energy and level density, reflecting the shell structure of nascent fragments at scission, is adequate to explain all observed effects.

### III. ANALYSIS OF PRESSION DECAY

We now come to the main point of this study: Is there, or can one expect, any evidence for GDR  $\gamma$  rays emitted by the  $^{252}\text{Cf}$  nucleus on its descent from the saddle to the scission point? Our calculation follows the prescription of Ref. [4]. The maximum excitation energy available at scission was obtained from

$$U_{\text{sc}}(A_{\text{frag}}) = Q(A_{\text{frag}}) - E_K(A_{\text{frag}}) - E^{\text{def}}(A_{\text{frag}}).$$

For example,  $U_{\text{sc}} = 10$  MeV for the average mass split of 108/144 using a measured total kinetic energy of 187 MeV [10] and estimating the total fragment deformation  $E^{\text{def}} = E_1^{\text{def}} + E_2^{\text{def}} = 22$  MeV [9, 17, 24]. The average deformation for the system during its descent to the scission point (which determines the splitting of the giant dipole energies) was estimated as  $\beta = 1.0$ . This corresponds to an axis ratio for an axially symmetric prolate system with  $R_{\text{min}}/R_{\text{max}} = 1/2.4$  consistent with the saddle-point shape calculated for a nonrotating charged liquid drop [25] as well as with the average shape obtained from the dynamical calculations of Nix and Sierk [6]. The average giant dipole  $\gamma$  energy for  $^{252}\text{Cf}$  was calculated from the droplet model [26] as  $\bar{E}_{\text{GDR}} = 10.5$  MeV. With a prolate deformation  $\beta = 1.0$  the GDR components have energies and strengths of  $E_1 = 5.7$  MeV,  $S_1 = 1/3$ ,  $E_2 = 12.9$  MeV,  $S_2 = 2/3$ . The GDR widths were taken as  $\Gamma_1 = 2.2$  MeV and  $\Gamma_2 = 4.6$  MeV, which corresponds to the experimental widths of the two GDR components built on the ground states of  $^{235,238}\text{U}$  [27]. The level density parameters used for the precession decay were calculated by CASCADE from the Dilg formula [28] which yields  $a = 34.85$  MeV $^{-1}$  and  $\Delta = -0.26$  MeV for  $^{252}\text{Cf}$ . These values were used for the entire excitation energy range ( $\leq 26$  MeV). (The CASCADE code's method of interpolating between low energy and high energy level density parameters produces incorrect decay rates for these low excitation energies.) It was furthermore assumed that the descent to the scission

point is described by an overdamped motion down a linear slope, so that the excitation energy increases linearly with time. The descent was then broken up into steps of constant energy gain  $\Delta U = 2$  MeV from  $U = 0$  to  $U = U_{\text{sc}}$ , each energy interval being held for a time interval  $\Delta t$ . This time scales with the energy dissipation of the system according to  $\Delta t = 2\gamma\Delta t_0$ , where  $\gamma$  is the normalized friction coefficient and  $\Delta t_0 = 4/U_{\text{sc}}(\text{sym}) \times 10^{-21}$  s. For each interval  $\Delta U$ , the particle and  $\gamma$  ray decay was calculated and the results added up. This was done for each fission-fragment mass split, and the result weighted with the probability of the respective mass split. Pre- and post-scission spectra were then added together.

The results are summarized in Fig. 4 which shows the precession  $\gamma$  spectra and the total calculated  $\gamma$ -ray energy spectra obtained for three different scission times, superimposed on the data of Ref. [1]. We also list the calculated precession neutron multiplicities. The available data [29–32] indicate an upper limit of  $\nu_{\text{sc}} \leq 0.4$ .

Using a time interval  $\tau_{\text{sc}} = 30 \times 10^{-21}$  s to reach the scission point (corresponding to full one-body dissipation) results in a precession neutron multiplicity of  $\nu_{\text{sc}} \approx 0$ , and a precession  $\gamma$  yield which is completely masked by the fission-fragment  $\gamma$  rays. Increasing the scission time scale by more than two orders of magnitude

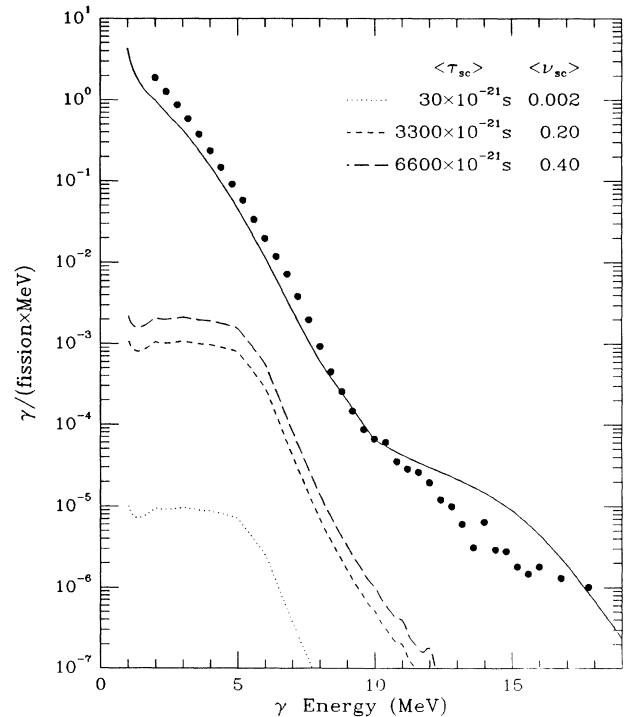


FIG. 4. The contribution from precession  $\gamma$  emission (dashed curves) is calculated for saddle-to-scission periods of  $\tau_{\text{sc}} = 30 \times 10^{-21}$  s,  $\tau_{\text{sc}} = 3300 \times 10^{-21}$  s, and  $\tau_{\text{sc}} = 6600 \times 10^{-21}$  s, which results in a predicted precession neutron multiplicity of  $\nu_{\text{sc}} = 0.002$ ,  $\nu_{\text{sc}} = 0.20$ , and  $\nu_{\text{sc}} = 0.4$ , respectively. The full drawn curve and the solid points represent the fission-fragment  $\gamma$  spectrum and the experimental data [1], respectively.

produces a precission neutron multiplicity at the experimental limit of  $\nu_{sc} \leq 0.4$ , but still yields no appreciable precission  $\gamma$  contribution. Accordingly, even when the precission spectrum is included, the angular correlation displays only the fission-fragment Doppler effects.

#### IV. SUMMARY

We find that statistical model calculations which are constrained by the detailed data on neutron emission in fission are able to describe the enhanced emission of 3 to 10 MeV  $\gamma$  rays which has been observed for the nearly symmetric fission component. Thus it appears that the recently proposed mechanism of coherent radiation from the shape vibrations of the nascent fragments is not required.

Within the constraints set by the precission neutron multiplicity and theoretically reasonable saddle-to-scission time scales, the model predicts that precission  $\gamma$  rays should be unobservable in the presence of fission-fragment  $\gamma$  rays. Thus, the strong  $\gamma$ -fission angular correlation reported for  $E_\gamma \sim 8$  to 12 MeV remains unexplained.

#### ACKNOWLEDGMENTS

We are indebted to J. Bacelar for extensive discussions on his experiment, and to H. van der Ploeg for providing us with his data and detector response function. This work was supported in part by the U.S. National Science Foundation.

- 
- [1] H. van der Ploeg, R. Postma, J. C. Bacelar, T. van den Berg, V. E. Jacob, J. R. Jongman, and A. van der Woude, *Phys. Rev. Lett.* **68**, 3145 (1992).
  - [2] P. Glässel, R. Schmidt-Fabian, D. Schwalm, D. Habs, and H. V. Helmdt, *Nucl. Phys. A* **502**, 315c (1989).
  - [3] A. Wiswesser, W. Pilz, and U. Jahnke, MPI für Kernphysik (Heidelberg) Annual Report 1991, p. 85.
  - [4] R. Butsch, D. J. Hofman, C. P. Montoya, P. Paul, and M. Thoennessen, *Phys. Rev. C* **44**, 1515 (1991).
  - [5] I. Diószegi, D. J. Hofman, C. P. Montoya, S. Schadmand, and P. Paul, *Phys. Rev. C* **46**, 627 (1992).
  - [6] J. R. Nix and A. J. Sierk, in *Proceedings of the International Symposium on Perspectives in Nuclear Physics*, Madras, India, 1987 (unpublished).
  - [7] F. Pühlhofer, *Nucl. Phys. A* **260**, 276 (1977).
  - [8] R. Butsch, M. Thoennessen, D. R. Chakrabarty, M. G. Herman, and P. Paul, *Phys. Rev. C* **41**, 1530 (1990).
  - [9] B. D. Wilkins, E. P. Steinberg, and R. R. Chasman, *Phys. Rev. C* **14**, 1832 (1976).
  - [10] H. W. Schmitt, J. H. Neiler, and F. J. Walter, *Phys. Rev.* **141**, 1146 (1966).
  - [11] C. Budtz-Jørgensen and H.-H. Knitter, *Nucl. Phys. A* **490**, 307 (1988).
  - [12] C. Signarbieux, R. Babinet, H. N. Niefenecker, and J. Poitou, in *Proceedings of the IAEA Symposium on the Physics and Chemistry of Fission*, Rochester, 1973 (IAEA, Vienna, 1974), p. 117.
  - [13] H. R. Bowman, J. C. D. Milton, S. G. Thomsons, and W. J. Swiatecki, *Phys. Rev.* **129**, 2133 (1963).
  - [14] R. Vandenbosch and J. R. Huizenga, *Nuclear Fission* (Academic, New York, 1973).
  - [15] R. K. Gupta, W. Scheid, and W. Greiner, *Phys. Rev. Lett.* **35**, 353 (1975).
  - [16] K. Skarsvag, *Phys. Rev. C* **22**, 638 (1980).
  - [17] R. W. Hasse, *Ann. Phys. (N.Y.)* **68**, 377 (1971) (see table A.III.b).
  - [18] H. Niefenecker, C. Signarbieux, R. Babinet, and J. Poitou, in [12], p. 117.
  - [19] D. R. Chakrabarty, S. Sen, M. Thoennessen, N. Alamanos, P. Paul, R. Schicker, J. Stachel, and J. J. Gaardhøje, *Phys. Rev. C* **36**, 1886 (1987).
  - [20] S. J. Luke, C. A. Gossett, and R. Vandenbosch, *Phys. Rev. C* **44**, 1548 (1991).
  - [21] J. Kasagi *et al.*, *Nucl. Phys. Soc. Jpn.* **58**, 620 (1989).
  - [22] F. S. Dietrich, J. C. Browne, W. J. O'Connell, and M. J. Kay, *Phys. Rev. C* **10**, 795 (1974).
  - [23] K. Dietrich and J. Bondorf, *Z. Phys. A* **343**, 191 (1992).
  - [24] H. Schultheiss and R. Schultheiss, *Phys. Rev. C* **18**, 1317 (1978).
  - [25] S. Cohen and W. J. Swiatecki, *Ann. Phys. (N.Y.)* **22**, 406 (1963).
  - [26] W. D. Myers, W. J. Swiatecki, T. Kodama, L. J. El-Jaick, and E. R. Hilf, *Phys. Rev. C* **15**, 2032 (1977).
  - [27] S. S. Dietrich and B. L. Berman, *At. Data Nucl. Data Tables* **38**, 199 (1988).
  - [28] W. Dilg, W. Schantl, H. Vonach, and M. Uhl, *Nucl. Phys. A* **217**, 269 (1973).
  - [29] E. A. Serëgina and P. P. D'yachenko, *Yad. Fiz.* **42**, 1337 (1985) [*Sov. J. Nucl. Phys.* **42**, 845 (1985)].
  - [30] V. M. Piksaikin, P. P. D'yachenko, and L. S. Kutsaeva, *Yad. Fiz.* **25**, 723 (1977) [*Sov. J. Nucl. Phys.* **25**, 385 (1977)].
  - [31] A. Gavron and Z. Fraenkel, *Phys. Rev. C* **9**, 632 (1974).
  - [32] H. R. Bowman, S. G. Thompson, J. C. D. Milton, and W. J. Swiatecki, *Phys. Rev.* **126**, 2120 (1962).